ARTICLE
Journal of Cellular Biochemistry 112:3002–3014 (2011)

Journal of Cellular Biochemistry

Comparative Proteome Analysis of 3T3-L1 Adipocyte Differentiation Using iTRAQ-Coupled 2D LC-MS/MS

Feng Ye,[1,2] Huoming Zhang,[3] Yi-Xuan Yang,[4] Huai-Dong Hu,[4] Siu Kwan Sze,[3] Wei Meng,[3] Jingru Qian,[3] Hong Ren,[4] Bao-Lin Yang,[1,2] Ming-Ying Luo,[1,2] Xiaoqiong Wu,[2] Wu Zhu,[1] Wei-Jun Cai,[1*] and Jian-Bin Tong[2*]

[1]*Department of Histology & Embryology, Xiangya School of Medicine, Central South University, Changsha, Hunan 410078, China*

[2]*Department of Anatomy & Neurobiology, Xiangya School of Medicine, Central South University, Changsha, Hunan 410078, China*

[3]*School of Biological Science, Nanyang Technological University, 60 Nanyang Drive, Singapore 637551, Singapore*

[4]*Key Laboratory of Molecular Biology for Infectious Diseases, Ministry of Education of China, The Second Affiliated Hospital, Chongqing Medical University, Chongqing 400010, China*

ABSTRACT

Adipose tissue is critical in obesity and type II diabetes. Blocking of adipocyte differentiation is one of the anti-obesity strategies targeting on strong rise in fat storage and secretion of adipokine(s). However, the molecular basis of adipocyte differentiation and its regulation remains obscure. Therefore, we exposed 3T3-L1 cell line to appropriate hormonal inducers as adipocyte differentiation model. Using iTRAQ-coupled 2D LC-MS/MS, a successfully exploited high-throughput proteomic technology, we nearly quantitated 1,000 protein species and found 106 significantly altered proteins during adipocyte differentiation. The great majority of differentially expressed proteins were related to metabolism enzymes, structural molecules, and proteins involved in signal transduction. In addition to previously reported differentially expressed molecules, more than 20 altered *proteins* previously unknown to be involved with adipogenic process were firstly revealed (e.g., HEXB, DPP7, PTTG1IP, PRDX5, EPDR1, SPNB2, STEAP3, TPP1, etc.). The partially differential proteins were verified by Western blot and/or real-time PCR analysis. Furthermore, the association of PCX and VDAC2, two altered proteins, with adipocyte conversion was analyzed using siRNA method, and the results showed that they could contribute considerably to adipogenesis. In conclusion, our data provide valuable information for further understanding of adipogenesis. J. Cell. Biochem. 112: 3002–3014, 2011.

KEY WORDS: 3T3-L1 ADIPOCYTES; PROTEOMICS; DIFFERENTIATION; iTRAQ

Obesity is one of the most frequent physiological disorders that is associated with a wide variety of conditions including type II diabetes, cardiovascular diseases and cancer [Thompson and Wolf, 2001]. It is characterized by excess of body fat mass, which is mostly stored in adipose tissue. There are indications that obesity is fast becoming a serious health problem worldwide [Bray and Tartaglia, 2000; Thompson and Wolf, 2001].

Accumulating evidence has indicated that adipocyte differentiation, an increase in fat cell *number*, plays an important role in obesity, and adipose tissue is a highly active endocrine organ capable of secreting a number of signal molecules called adipokines (including leptin, adiponectin, resistin, etc.) [Bray and Tartaglia, 2000; Rosen and Spiegelman, 2006; Trujillo and Scherer, 2006; Molina et al., 2009; Ye et al., 2010]. Leptin has actions in the metabolism, development, immune system, reproduction, hemopoiesis, angiogenesis, and bone formation [Bornstein et al., 2000; Cock and Auwerx, 2003; Rondinone, 2006; Than et al., 2010]. Resistin participates in obesity, type II diabetes, and inflammation-

Abbreviations used: 2D, two-dimensional; LC, liquid chromatography; MS, mass spectrometry; iTRAQ, isobaric tags for relative and absolute quantification; SILAC, stable isotope labeling with amino acids in cell culture; DIGE, differential gel electrophoresis; ICAT, isotope-coded affinity tag.

The authors declare that there is no conflict of interest that could be perceived as prejudicing the impartiality of this scientific work.

Grant sponsor: Natural Sciences Funds of China; Grant numbers: 30971532, 30771134, 30930082, 30900507, 30801348.

*Correspondence to: Prof. Wei-Jun Cai, MD, PhD, Jian-Bin Tong, MD, PhD, 172 Tong-Zhi-Po Road, Changsha, Hunan 410078, P.R. China. E-mail: wjcai@yahoo.com, jianbintong@yahoo.com

Received 15 March 2011; Accepted 3 June 2011 • DOI 10.1002/jcb.23223 • © 2011 Wiley-Liss, Inc.

Published online 15 June 2011 in Wiley Online Library (wileyonlinelibrary.com).

related diseases. In a summary, adipose tissue plays key roles in the regulation of energy homeostasis, lipoprotein metabolism and other physiological functions via adipokines [Miner, 2004; Rondinone, 2006; Rosen and Spiegelman, 2006; Trujillo and Scherer, 2006; Lago et al., 2007, 2009]. A plenty of adipokines were consequently released to play multifaceted roles through both central and peripheral mechanisms due to the excessive increase of sheer number and volume of adipocytes. Targeting on adipocyte differentiation became one approach among the anti-obesity and related diseases strategies targeting on strong rise in fat storage and secretion of adipokine(s) [Bray and Tartaglia, 2000; Rosen and Spiegelman, 2006; Trujillo and Scherer, 2006; Kim et al., 2008]. Previous studies demonstrated that many transcription factors and metabolism enzymes are altered during various stages of adipogenesis and play roles in adipocyte differentiation (e.g., CCAAT/enhancer binding proteins (C/EBPs), cAMP response element-binding protein (CREB), peroxisome proliferator-activated receptor (PPAR)-gamma, fatty acid synthase (FAS), pyruvate carboxylase (PCX), superoxide dismutase (SOD), and lipoprotein lipase (LPL) that are differentially expressed during adipocyte differentiation). Indeed, differentiation of adipocyte may be regulated by a complex network of adipogenic transcription factors [Shao and Lazar, 1997; Zhou et al., 1999; Hackl et al., 2005], and matured adipocytes act as endocrine cells [Miner, 2004]. These factors affect each other and regulate the expression of adipokines positively or negatively [Zhou et al., 1999; Hackl et al., 2005].

However, until now, the mechanisms and regulation of adipocyte differentiation and secretion are inadequately understood. Several studies using proteomic approaches have been reported. These studies have used 2D electrophoresis technology [Renes et al., 2005; Atiar Rahman et al., 2008; Kim et al., 2009; Choi et al., 2004] or SILAC [Molina et al., 2009], and might have missed many *low abundance* proteins that are important to the adipogenic process. Recently, there has been great progress in comparative proteomic approaches, including DIGE, iTRAQ, ^{18}O, ICAT, and SILAC. Among these methods, iTRAQ technology has gained great popularity in quantitative proteomics applications due to its high sensitivity, accurate quantitation and reproducibility [Hu et al., 2010; Zhang et al., 2011]. Murine 3T3-L1 cells, a most frequent adipogenesis model, are used to study adipocytes in vitro. To our best knowledge, there is no report that profiled proteome during 3T3-L1 adipocyte differentiation using iTRAQ-coupled 2D LC-MS/MS. The present study was designed to find proteins involved in regulation of adipocyte differentiation and secretion of adipokine(s) using this high-throughput proteomic technology. We screened 106 differentially expressed proteins during adipocyte differentiation. This systematic proteomic approach led to the discovery of novel proteins targeting on obesity.

MATERIALS AND METHODS

REAGENTS

The iTRAQ kit was purchased from Applied Biosystems Company (MA). Two-dimentional Quant Kit was purchased from GE Healthcare (WI). Sequence grade modified Trypsin was purchased from Promega (WI). Bromophenol blue, Bis, TEMED, coomassie brilliant blue G-250, low molecular weight marker, Tris-base, nitrocellulose membrane, and protein assay kit based on Bradford method were purchased from Bio-Rad Company (CA). Polyclonal antibodies, secondary antibodies, and siRNA kits were purchased from Santa Cruz Biotechnology (CA). Pierce chemiluminescent substrate kit was purchased from Thermo Scientific (USA). Lipofectamine 2000 reagent was obtained from Invitrogen Corporation (Carlsbad, CA). Commercial triglyceride kit was purchased from Zhongsheng Company (Beijing, China). Unless otherwise noted, all other reagents were from Sigma Company (USA).

CELL CULTURE AND DIFFERENTIATION

Murine 3T3-L1 fibroblasts (American Type Culture Collection, MD) were initially cultured in DMEM medium (Gibco, Rockville, MD) supplemented with 10% heat-inactivated bovine calf serum (Gibco) and 1% penicillin–streptomycin (Gibco) at 37°C in a humidified atmosphere of 5% CO_2/95% air. Differentiation of 3T3-L1 fibroblasts to adipocytes was induced similarly as previously described [Shao and Lazar, 1997]. After 3T3-L1 fibroblasts reached confluence for 2 days (referred as day 0), cells were cultured in the differentiation medium for 2 days, which is DMEM medium supplemented with 10% fetal bovine serum (FBS), 1 μM dexamethasone, 10 μg/ml insulin, and 0.5 mM isobutyl-1-methylxanthine. The cells were then maintained in the medium containing 10% FBS and 10 μg/ml insulin for 2 days and replenished with the DMEM containing 10% FBS. Differentiation was monitored by the visual appearance of fat droplets in the cells. In this series of experiments, we set two groups: (1) 3T3-LI fibroblasts. They were collected after cells reached confluence; (2) 3T3-LI adipocytes. On day 10 of differentiation, cells were harvested. The samples prepared for protein or total RNA extraction. At the same time, adipogenesis was evaluated by Oil Red staining (a specific lipid staining) and triglyceride analysis. Oil Red O staining was used to monitor the adipogenic process. It was performed as previously described with minor modifications [Akerblad et al., 2005]. In brief, cells were washed twice in ice-cold PBS and fixed in PBS containing 4% formaldehyde. After a single wash in water, cells were stained with Oil Red O for 30 min. Oil Red O was prepared by diluting a stock solution [0.6 g of Oil Red O (Sigma Company) in 100 ml of isopropanol] with water (3:2) followed by filtration. After elution of Oil Red O with isopropanol, the extent of adipocyte differentiation was quantitated by determining the amount of extracted dye as measured by the optimal absorbance at 520 nm. The triglyceride produced by the cells was taken as an index of adipocyte differentiation. 3T3-L1 cells were collected and homogenized by sonication. Cellular triglyceride content was determined by using Triglyceride *GPO-POD* Assay Kit (Zhongsheng Company) according to the manufacturer's protocol. This procedure involves enzymatic hydrolysis by lipase of the triglycerides to glycerol and free fatty acids. The increase in absorbance at 500 nm is directly proportional to triglyceride concentration of the sample.

PROTEIN SAMPLES PREPARATION

The cells were collected and then re-suspended in lysis buffer (0.5 M triethylammonium bicarbonate (TEAB) and 1% SDS) at 4°C. The cell

lysate was subjected to intermittent sonication using a Vibra Cell™ high intensity ultrasonic processor (Jencon, Leighton Buzzard, Bedfordshire, UK). The remaining unbroken cells and debris were removed by centrifugation at 4°C at 12,000*g* for 10 min. Protein concentration of cleared lysates was quantified using the 2D Quant Kit (GE Healthcare). A standard curve was made using BSA as a control.

PROTEIN DIGESTION AND iTRAQ LABELING

Each sample was equally divided into two tubes. The proteins were reduced with 5 mM tris-carboxyethyl phosphine hydrochloride (TCEP) for 1 h at 37°C, alkylated with 10 mM methylethanethiosulfonate (MMTS) for 20 min at room temperature (RT); and then diluted 10 times with deionized water prior to digestion with sequence grade modified trypsin (Promega) overnight at 37°C at a 1 part trypsin to 50 part protein mass ratio and then dried using a Speedvac (Thermo Electron). Peptides generated were labeled with iTRAQ reagents according to the manufacturer's protocol (Applied Biosystems Company). Briefly, digested proteins were reconstituted in 30 μl of 0.5 M TEAB buffer and mixed with 70 μl of ethanol-suspended iTRAQ reagents (one iTRAQ reporter tag per protein sample). The samples were labeled with the respective tags as followed: control 3T3-LI fibroblasts = iTRAQ 114; 3T3-LI adipocytes = iTRAQ 115. Labeling reactions were carried out for 1 h at RT before all the samples were mixed into a tube and dried using a Speedvac. To increase the coverage of protein identification and/or the confidence of the data generated, independent two experiments were performed.

STRONG CATION EXCHANGE FRACTIONATION

The combined iTRAQ labeled samples were reconstituted with buffer A (10 mM KH_2PO_4, pH 3.0, 25%, v/v, acetonitrile), and loaded into a PolySULFOETHYL A column (200 mm length × 4.6 mm ID, 200-Å pore size, 5 μm particle size) (PolyLC, MD) on a prominence HPLC system (Shimadzu, Kyoto, Japan). The sample was fractionated using a gradient of 100% buffer A for 5 min, 5–30% buffer B (10 mM KH_2PO_4, pH 3.0, 500 mM KCl, and 25%, v/v, acetonitrile) for 40 min, 30–100% buffer B for 5 min, and finally 100% buffer B for 5 min, at a constant flow rate of 1 ml/min for a total of 1 h. The eluted fractions were monitored through a UV detector at 214 nm wavelength. Fractions were collected at 1-min intervals and consecutive fractions with low peak intensity were combined. Finally a total of 20 fractions were obtained and dried in a Speedvac (Thermo Electron). Each fraction was reconstituted in 0.1% trifluoroacetic acid and desalted using a Sep-Pak C-18 SPE cartridge (Waters, Milford, MA). Desalted samples were dried in a Speedvac (Thermo Electron) and stored at −20°C prior to mass spectrometric analysis.

MASS SPECTROMETRIC ANALYSIS USING Q-STAR

Each dried fraction was reconstituted in 100 μl of 0.1% formic acid and 2% acetonitrile and then analyzed times using a Q-Star Elite mass spectrometer (Applied Biosystems Company; MDS-Sciex), coupled to a prominence HPLC system (Shimadzu). For each analysis, 100 μl of peptide mixture was injected in a Zorbax peptide trap (Agilent, CA) and separated on a nanobored C18 column with a picofrit nanospray tip (75 μm ID × 15 cm, 5 μm particles) (New Objectives, Wubrun, MA). The separation was performed at a constant flow rate of 0.3 μl/min with a 2 h gradient. The mass spectrometer was set to perform data acquisition in the positive ion mode, with a selected mass range of 300–2,000 m/z. Peptides with +2 to +4 charge states were selected for MS/MS and the time of summation of MS/MS events was set to 2 s. The three most abundantly charged peptides above a 5-count threshold were selected for MS/MS and dynamically excluded for 30 s with ±30 mmu mass tolerance.

DATA ANALYSIS AND INTERPRETATION

Peptide and protein identification were performed using ProteinPilot™ Software v2.0.1 (Applied Biosystems Company) by searching data against the International Protein Index (IPI) mouse database. The Paragon algorithm in ProteinPilot software was used whereby trypsin was selected as the digestion agent and cysteine modification of methylethanethiosulfonate. The search also allows for the possibilities of more than 80 biological modifications using the BLOSUM 62 matrix. All proteins reported had at least two unique peptide matches with iTRAQ ratios, and at least one of them must have an expectation value <0.05. Finally, a concatenated target-decoy database search strategy was also performed to estimate the rate of false positives and was determined to be <1% for the current analysis. To account for small differences in protein loading, all protein ratios have been normalized using the overall ratios for all proteins in the sample, as recommended by Applied Biosystems Company.

WESTERN BLOT ANALYSIS

Total protein lysates extracted from the experiments as described above for the LC/MS /MS analysis were used for the Western blot analysis. Specifically, total proteins from each of the two types of cells were separated on the SDS–polyacrylamide gels using a Mini-Protean Tetra cell, and then transblotted onto the nitrocellulose membrane using a Mini-Transblot apparatus at 4°C (Bio-Rad Lab). The protein signals were amplified using Pierce Qentix Western blot signal enhancer kit (Thermo Scientific), followed by blocking for 2 h at 4°C with 5% non-fat dry milk in TBST buffer (10 mmol/L Tris, 150 mmol/L NaCl, and 0.05% Tween-20, pH 7.5), followed by 4–6 h of incubation with specific primary antibodies (see below; 1:100–800; Santa Cruz Biotechnology) in TBST buffer containing 5% non-fat dry milk at RT. After washing three times with TBST buffer, the membranes were incubated with a secondary antibody-conjugated horseradish peroxidase (1:3,000–6,000; Thermo Scientific) for 4–5 h at RT. After the membranes were washed three times in TBST buffer, the reactions were visualized with Pierce chemiluminescent substrate kit (Thermo Scientific). The results were then scanned using Bio-Rad's Densitometer and analyzed using Bio-Rad's Quality One software. The antibodies used in this study were as follows: (1) Destrin; (2) Nucleolin; (3) Zyx protein; (4) Transgelin 2; (5) β-actin; (6) Voltage-dependent anion-selective channel protein 2 (VDAC2); (7) Voltage-dependent anion-selective channel protein 3 (VDAC3); (8) Cytochrome b5; and (9) PCX. All samples were normalized by protein content that was measured using the protein assay kit (Bio-Rad Lab) based on Bradford method.

Intracellular β-actin served as a loading control. Independent triplicate experiments were performed.

REAL-TIME PCR

Cells were cultured for RNA isolation using RNeasy mini kit (Qiagen). The iSCRIPT One-step RT-PCR kit (Bio-Rad) was used for the real-time quantification of RNA targets. SYBR Green was used as a dye to emit the fluorescence signal. The following primer sequences were specific to cDNAs which displayed changes in the respective protein level. The specific primers for Annexin A1 were 5′-AAGTAGGAAAGTTGCTTTGG-3′ (sense) and 5′-AAGTGACTTGCTTATGGGGC-3′ (antisense), for Cytochrome b5 were 5′-GTTTCTCGAAGAGCATCCTG-3′ (sense) and 5′-GAAGGCTTGGCTATCTTTGA-3′ (antisense), for EEF1A1 were 5′-TAATCAGTGGTGGAAGAACGG-3′ (sense) and 5′-AATGGTCCACAACATTCTTTCC-3′ (antisense), for VDAC2 were 5′-GGCTCACGTATGTGCAGTTAC-3′ (sense) and 5′-TATTGTAATCTCAAAGACCTCG-3′ (antisense), for Ribosomal protein SA were 5′-CATCCAGCAGTTCCCCAC-3′ (sense) and 5′-CAGCAGATCAGGACCACTCA-3′ (antisense), for Nucleolin were 5′-ACTTAAAGGGATCCCTTTAA-3′ (sense) and 5′-AGGCATGGCATTCTCCTGGCA-3′ (antisense), for Transgelin 2 were 5′-GCAGCAGAAGATTGAGAAGC-3′ (sense) and 5′-ATCTTCTTTACTGGGGCCTG-3′ (antisense), and for β-actin were 5′-CCCCATTGAACATGGCATTG-3′ (sense) and 5′-ACGACCAGAGGCATACAGG-3′ (antisense), respectively. These primers were designed to amplify these products around 150–300 bp in size to reduce non-specific-binding of SYBR Green. Quantification was performed by calculating the fluorescence density during the amplification cycle. The disassociation analysis was routinely carried out by acquiring fluorescent reading for one degree increase from 55 to 95°C. The data including amplification analysis, melting curve analysis, and threshold cycle number were provided automatically by optical system software (Bio-Rad). Real-time PCR analysis was repeated at least three times.

ADMINISTRATION OF PCX OR VDAC2 siRNA TO CELLS

The cells were transfected with PCX siRNA (sc-45532), or VDAC2 siRNA (sc-42358) (Santa Cruz Biotechnology) using Lipofectamine 2000 reagent according to the manufacturer's instructions. Control siRNA (sc-37007, Santa Cruz Biotechnology) served as a negative control according to the manufacturer's protocol. Briefly, cells were plated into six-well plates. After 3T3-L1 fibroblasts reached confluence for 2 days, they were transfected with specific siRNA, and control siRNA after a pre-incubation for 15 min with siRNA transfection reagent in siRNA transfection medium. After 6 h of transfection, the medium was replaced with growth medium containing 10% fetal calf serum. After 3 days, repeated above procedures until day 10 of differentiation. Adipocyte conversion was evaluated by the visual appearance of fat droplets in the cells, Oil Red staining and triglyceride analysis. PCX or VDAC2 expression level was determined by Western blot analysis described above.

STATISTICAL ANALYSIS

In this study, results are expressed as means ± SEM. All values were evaluated by the unpaired Student's *t*-test. $P < 0.05$ was considered to be statistically significant.

RESULTS

ADIPOCYTE DIFFERENTIATION

On day 10 of differentiation, more than 75% of the cells showed adipogenic conversion characterized by visible fat droplets inside the cells (data not shown). The total amount of intracellular Oil Red staining in 3T3-L1 adipocytes was strongly increased compared with control fibroblasts (2.80 ± 0.1137 vs. 0.158 ± 0.012, $P < 0.001$; Table I). The results were confirmed by measurement of cellular triglyceride. It is consistent with Oil Red staining (Table I).

iTRAQ ANALYSIS OF DIFFERENTIALLY EXPRESSED PROTEINS BETWEEN FIBROBLAST AND ADIPOCYTE

Peptides generated from trypsin digestion of fibroblast and adipocyte proteins were labeled at their free amine sites using the isobaric mass tag labels, mixed together and analyzed by reverse phase liquid chromatography coupled to mass spectrometry. Upon collision-induced dissociation, the parent peptides were broken up and the associated isobaric mass tags were released. The dissociation of the parent peptide yielded a characteristic mass fragmentation pattern that enabled identification of the parent protein by comparing this fragmentation fingerprint to theoretical digests of proteins. Additionally comparative peptide data could be obtained for multiple proteins from one experiment. This process reduces any variability of peptide measurement for samples. We nearly identified 1,600 proteins from each of the two independent experiments conducted. Among them, more than 900 proteins were quantified (920 and 935 proteins, respectively). Testing for multiple comparisons from quantitative information eventually led to 106 differentially expressed proteins including 52 up-regulated proteins and 54 down-regulated proteins (Table II). The following criteria were required to consider as a differentially expressed protein: two or more high confidence (>95%) unique peptides had to be identified, fold changes had to be >1.4, and $P < 0.05$ in the Protein Quant. These differential proteins were subsequently classified into six groups according to their cellular functions (Fig. 1), based on the UniProt Knowledgebase (Swiss-Prot or TrEMBL http://www.uniprot.org/). These proteins are involved in cellular metabolism (45), cellular structure (including cytoskeletal proteins, molecular chaperone) (32), cell signaling pathway (including transcription factor) (15), cell secretion (3), calcium function (6), and unknown function (5). Figure 2 illustrates the representative MS/MS of VDAC2 and β-actin, respectively, showing their differential expression levels. The expression levels of VDAC2 were significantly increased compared to pre-adipocyte, whereas β-actin expression remained

TABLE I. Parameters of 3T3-LI Fibroblasts and Adipocyte (n = 7 Each Group)

Name	3T3-LI fibroblasts	3T3-LI adipocytes
Oil Red staining (OD 520 nm)	0.158 ± 0.012	$2.80 \pm 0.1137^{***}$
Triglyceride (mg/mg)	0.229 ± 0.017	$1.812 \pm 0.08^{***}$

Data are expressed as means ± SEM. Triglyceride was showed as mg cellular triglyceride per mg of total cellular protein. Statistical significance was determined by analysis of variance, followed by Student's unpaired *t*-test. The acceptable level of significance was $^{**}P < 0.01$, $^{***}P < 0.001$ versus 3T3-LI fibroblasts.

TABLE II. iTRAQ Analysis of Differentially Expressed Proteins in the Adipocytes Compared to Fibroblasts

Number	Accession	Gene	Protein	115:114	*P*-value, 115:114	Function
1	IPI00115530.1	HEXB	Beta-hexosaminidase beta chain precursor	7.30*	3.09E−06	Carbohydrate metabolic process, cellular calcium ion homeostasis, beta-*N*-acetylglucosaminidase activity, beta-*N*-acetylhexosaminidase activity
2	IPI00377642.2	PTTG1IP	Pituitary tumor-transforming gene 1 protein-interacting protein precursor	6.18*	0.0003	Protein import into nucleus, molecular function unknown
3	IPI00387497.1	DPP7	Dipeptidylpeptidase 7	5.30*	1.2E−03	Metabolic enzymes
4	IPI00116705.5	FABP4	Fatty acid-binding protein, adipocyte	4.16	0.0015	Binding, lipid binding, brown fat cell differentiation, cellular response to lithium ion
5	IPI00165730.4	1300012G16Rik	Isoform 1 of putative phospholipase B-like 2 precursor	3.54*	1.9E−03	Metabolic enzymes
6	IPI00221426.3	GNS	*N*-acetylglucosamine-6-sulfatase precursor	3.20	1.6E−03	Metabolic enzymes
7	IPI00316989.7	EPDR1	Isoform 1 of mammalian ependymin-related protein 1 precursor	3.08*	1.8E−04	Secreted protein
8	IPI00130661.1	TPP1	Tripeptidyl-peptidase 1 precursor	3.00*	2.7E−02	Metabolic enzymes, lysosomal serine protease with tripeptidyl-peptidase I activity
9	IPI00381303.5	MAN2B1	Lysosomal alpha-mannosidase precursor	2.78	1.0E−03	Metabolic enzymes, necessary for the catabolism of N-linked carbohydrates released during glycoprotein turnover
10	IPI00306723.3	CEBPZ	CCAAT/enhancer-binding protein zeta	2.67	0.005	Regulation of transcription
11	IPI00226563.4	TTYH3	Isoform 1 of protein tweety homolog 3	2.65	1.3E−02	Ca(2+) signal transduction
12	IPI00117842.2	MAN2B2	Epididymis-specific alpha-mannosidase precursor	2.64	2.3E−03	Plays an important role in the early step of spermatogenesis
13	IPI00755338.2	LPL	Lipoprotein lipase	2.53	0.031961	Fatty acid biosynthetic process, lipid catabolic process, catalytic activity, heparin binding
14	IPI00134961.1	ACADM	Medium-chain specific acyl-CoA dehydrogenase, mitochondrial precursor	2.48*	0.0004	Cardiac muscle cell differentiation, carnitine biosynthetic process, acyl-CoA dehydrogenase activity
15	IPI00230113.5	CYB5	Cytochrome b5	2.43	5.1E−03	Cellular structure, It is also involved in several steps of the sterol biosynthesis pathway, particularly in the C-5 double bond introduction during the C-5 desaturation
16	IPI00653231.1	SFXN3	Sideroflexin 3, full insert sequence	2.41	8.7E−03	Cation transmembrane transporter activity
17	IPI00111960.2	GAA	Lysosomal alpha-glucosidase precursor	2.40	4.1E−03	Essential for the degradation of glycogen to glucose in lysosomes
18	IPI00223713.5	HIST1H1C	Histone H1.2	2.37	1.5E−06	The condensation of nucleosome chains into higher order structures
19	IPI00113389.5	NIBAN	Niban protein	2.36*	1.6E−03	Molecular function unknown, positive regulation of protein phosphorylation
20	IPI00132314.1	NUCB1	Nucleobindin-1 precursor	2.35*	1.0E−03	Calcium-binding protein, calcium homeostasis
21	IPI00113517.1	CTSB	Cathepsin B precursor	2.30	5.1E−03	Metabolic enzymes, tumor invasion and metastasis
22	IPI00114710.2	PCX	Pyruvate carboxylase	2.26	4.2E−05	Metabolic enzymes
23	IPI00122547.1	VDAC2	Voltage-dependent anion-selective channel protein 2	2.22	2.6E−04	Cellular structure
24	IPI00116896.1	MT-ATP8	ATP synthase protein 8	2.19	5.3E−03	Metabolic enzymes, ATP synthase
25	IPI00223092.5	HADHA	Trifunctional enzyme subunit alpha, mitochondrial precursor	2.14	6.0E−05	Metabolic enzymes, bifunctional subunit
26	IPI00318614.9	IDH2	Isocitrate dehydrogenase [NADP], mitochondrial precursor	2.07	0.0056	Glyoxylate cycle, isocitrate metabolic process
27	IPI00380136.3	LOXL1	Lysyl oxidase homolog 1 precursor	2.07	1.1E−02	Metabolic enzymes, active on elastin and collagen substrates
28	IPI00115626.1	PPAP2B	Lipid phosphate phosphohydrolase 3	2.066	0.0075	Catalytic activity, hydrolase activity, blood vessel development, canonical Wnt receptor signaling pathway
29	IPI00877201.1	CREB1	cAMP responsive element binding protein 1 isoform C	2.06	0.002	DNA binding, double-stranded DNA binding
30	IPI00314726.3	NAGLU	Alpha-*N*-acetylglucosaminidase	2.04	4.4E−02	Metabolic enzymes
31	IPI00128450.1	MBC2	Isoform 1 of extended-synaptotagmin-1	2.03*	9.4E−03	Calcium-regulated intrinsic membrane protein
32	IPI00620256.3	LMNA	Isoform A of lamin-A/C	1.99	3.6E−17	Cellular structure
33	IPI00230540.1	VDAC1	Isoform Mt-VDAC1 of voltage-dependent anion-selective channel protein 1	1.96*	8.7E−06	Cellular structure, signal transduction
34	IPI00330497.4	KANK2	Isoform 1 of KN motif and ankyrin repeat domain-containing protein 2	1.96*	2.2E−03	Molecular function unknown, negative regulation of stress fiber assembly
35	IPI00828222.1	FBN1	Mutant fibrillin-1	1.92*	3.9E−02	Calcium ion binding, chitin binding
36	IPI00620222.2	MYO1C	Isoform A of myosin-Ic	1.85	7.1E−03	Intracellular movements
37	IPI00319830.7	SPNB2	Isoform 1 of spectrin beta chain, brain 1	1.76*	7.3E−09	Secretion, interacts with calmodulin in a calcium-dependent manner and is thus candidate for the calcium-dependent movement of the cytoskeleton at the membrane

(*Continued*)

TABLE II. (*Continued*)

Number	Accession	Gene	Protein	115:114	*P*-value, 115:114	Function
38	IPI00116074.1	ACO2	Aconitate hydratase, mitochondrial precursor	1.76	2.0E−04	Catalytic activity
39	IPI00606510.1	PCCB	Propionyl-CoA carboxylase beta chain, mitochondrial precursor	1.76	3.1E−02	Catalytic activity
40	IPI00330941.3	STEAP3	Isoform 2 of metalloreductase STEAP3	1.75*	2.4E−02	Signal transduction, may play a role downstream of p53/TP53 to interface apoptosis and cell cycle progression. indirectly involved in exosome secretion by facilitating the secretion of proteins such as TCTP
41	IPI00319973.3	PGRMC1	Membrane-associated progesterone receptor component 1	1.74	6.4E−03	Cellular structure, receptor for progesterone
42	IPI00129571.3	COl3A1	Collagen alpha-1(III) chain precursor	1.73	1.1E−06	Cellular structure, collagen type III occurs in most soft connective tissues
43	IPI00848492.1	LOC10045699	Similar to electron transferring flavoprotein, beta polypeptide isoform 2	1.73*	2.4E−04	Molecular function unknown
44	IPI00555055.3	H2AFV	Histone H2AV	1.71	1.4E−02	Cellular structure, cell division
45	IPI00876341.1	VDAC3	Voltage-dependent anion-selective channel protein 3	1.71*	5.9E−04	Cellular structure, forms a channel
46	IPI00468203.3	ANXA2	Annexin A2	1.67	5.0E−09	Cellular structure
47	IPI00130589.8	SOD1	Superoxide dismutase	1.65	1.0E−02	Destroys radicals which are normally produced within the cells and which are toxic to biological systems
48	IPI00886077.1	PRDX5	Prdx5 protein	1.65*	3.8E−03	Oxidoreductase activity
49	IPI00658539.1	CTSA	Cathepsin A isoform a	1.62	4.2E−02	The activity of beta-galactosidase and neuraminidase, carboxypeptidase and can deamidate tachykinins. Catalytic activity
50	IPI00653158.1	ACAA2	14 days embryo liver cDNA, RIKEN full length enriched library, clone: I530029G20 product: acetyl	1.61	9.7E−03	Metabolic enzymes
51	IPI00399958.3	CALU	Calumenin isoform 2	1.59*	1.4E−03	Calcium ion binding
52	IPI00223987.1	LNPEP	Leucyl-cystinyl aminopeptidase	1.59	4.3E−02	Metabolic enzymes, aminopeptidase activity, angiotensin receptor activity, degrades peptide hormones maintaining homeostasis during pregnancy
53	IPI00830884.1	TPM1	33 kDa protein	0.70	2.3E−02	Cellular structure, muscle contraction stabilizing cytoskeleton actin filaments
54	IPI00224740.6	PFN1	Profilin-1	0.69	3.3E−03	Binds to actin and affects the structure of the cytoskeleton, signal transduction it inhibits the formation of IP3 and DG
55	IPI00457852.3	EG432502	Similar to ribosomal protein L6	0.67*	1.9E−04	Molecular function unknown
56	IPI00230395.5	ANXAL	Annexin A1	0.66	3.5E−05	Membrane fusion and exocytosis, this protein regulates phospholipase A2 activity
57	IPI00317794.5	NCL	Nucleolin	0.65	4.4E−04	Cellular structure, transcription factor
58	IPI00474446.4	EIF2S1	Eukaryotic translation initiation factor 2 subunit 1	0.64	2.9E−02	Cellular structure, protein synthesis
59	IPI00856927.1	RPS19	23 kDa protein	0.64*	1.2E−02	Protein binding erythrocyte differentiation gas transport
60	IPI00626106.3	TAGLN2	Transgelin 2	0.64	6.2E−03	Calponin family
61	IPI00130883.1	RBM3	Putative RNA-binding protein 3	0.63	2.7E−02	Cellular structure
62	IPI00874931.1	FUBP1	Isoform 1 of Far upstream element-binding protein 1	0.63	2.8E−02	Transcription factor
63	IPI00331552.4	PABPC1	Poly A binding protein, cytoplasmic 1, full insert sequence	0.62	9.9E−04	Cellular structure, transcription factor
64	IPI00454016.5	MAT2A	*S*-adenosylmethionine synthetase isoform type-2	0.62	5.1E−03	Catalyzes the formation of *S*-adenosylmethionine
65	IPI00849793.1	RP112	60S ribosomal protein L12	0.61	1.3E−02	Binds directly to 26S ribosomal RNA
66	IPI00626628.1	RP127A	EG665189 ribosomal protein L27a	0.61	2.3E−02	Cellular structure
67	IPI00462445.2	NEDD4	E3 ubiquitin-protein ligase NEDD4	0.61*	3.7E−03	E3 ubiquitin-protein ligase which accepts ubiquitin from an E2 ubiquitin-conjugating enzyme in the form of a thioester and then directly transfers the ubiquitin to targeted substrates Involved in the embryonic development and differentiation of the central nervous system
68	IPI00263863.8	HSPE1	10 kDa heat shock protein, mitochondrial	0.61*	1.1E−03	Molecular chaperone, mitochondrial protein biogenesis
69	IPI00473728.1	RP114	Ribosomal protein L14, cytosolic homolog	0.60	5.9E−03	Cellular structure
70	IPI00136912.1	SRM	Spermidine synthase	0.59	3.2E−04	Metabolic enzymes, catalytic activity, spermidine synthase activity, *S*-adenosylmethioninamine + putrescine = 5′-*S*-methyl-5′-thioadenosine + spermidine
71	IPI00314748.7	WDR1	WD repeat-containing protein 1	0.58	5.2E−04	Induces disassembly of actin filaments

(*Continued*)

TABLE II. (*Continued*)

Number	Accession	Gene	Protein	115:114	*P*-value, 115:114	Function
72	IPI00315488.1	RARS	Arginyl-tRNA synthetase, cytoplasmic	0.57	4.0E−04	Aminoacyl-tRNA ligase activity, arginine binding. ATP + L-arginine + tRNA(Arg) = AMP + diphosphate + L-arginyl-tRNA(Arg)
73	IPI00752985.1	EG666501	EG666738 similar to ribosomal protein L23a	0.57	1.4E−02	Cellular structure
74	IPI00467296.2	PFDN1	Prefoldin 1	0.57	3.3E−02	Binds specifically to cytosolic chaperonin (c-CPN) and transfers target proteins to it, binds to nascent polypeptide chain and promotes folding in an environment in which there are many competing pathways for non-native proteins
75	IPI00116277.3	CCT4	T-complex protein 1 subunit delta	0.56	1.1E−03	Molecular chaperone
76	IPI00321308.4	AARS	Alanyl-tRNA synthetase, cytoplasmic	0.56	8.0E−03	ATP + L-alanine + tRNA(Ala) = AMP + diphosphate + L-alanyl-tRNA(Ala)
77	IPI00122928.1	TUBB6	Tubulin beta-6 chain	0.56	2.7E−02	Cellular structure
78	IPI00458337.4	29 kDa protein	29 kDa protein	0.55	5.9E−05	Molecular function unknown
79	IPI00112555.3	GARS	Glycyl-tRNA synthetase	0.55	1.8E−02	ATP + glycine + tRNA(Gly) = AMP + diphosphate + glycyl-tRNA(Gly).
80	IPI00223757.4	AKR1B3	Aldose reductase	0.55	1.9E−02	Catalytic activity
81	IPI00277930.6	CAPG	Capping protein (actin filament), gelsolin	0.54*	3.3E−04	Calcium-sensitive protein, macrophage function regulating cytoplasmic and/or nuclear structures bind DNA
82	IPI00845840.1	PKM2	Isoform M1 of pyruvate kinase isozymes M1/M2	0.54	4.5E−03	Catalytic activity
83	IPI00850840.1	RPSA	Ribosomal protein SA	0.53	5.2E−04	Enables malignant tumor cells to penetrate laminin tissue and vessel barriers, activates precursor thymic anti-OFA/iLRP specific cytotoxic T cell. May induce CD8 T-suppressor cells secreting IL-10
84	IPI00408218.1	ZYX	Zyx protein	0.52	1.2E−02	Adhesion plaque protein, transcription factor
85	IPI00127942.4	DSTN	Destrin	0.51	3.4E−04	Actin-depolymerizing protein
86	IPI00469268.5	CCT8	T-complex protein 1 subunit theta	0.51	4.2E−06	Molecular chaperone
87	IPI00409918.1	EIF4A2	Isoform 2 of eukaryotic initiation factor 4A-II	0.51	9.3E−05	Transcription factor, cellular structure
88	IPI00134621.3	RAN	LOC100045999 GTP-binding nuclear protein Ran	0.50	2.0E−03	GTP-binding protein, transcription factor, involved in chromatin condensation and control of cell cycle
89	IPI00223415.3	NARS	Activated spleen cDNA, RIKEN full length enriched library, clone: F830225J05 product: asparaginyl-tRNA synthetase, full insert sequence	0.49	8.1E−03	Catalytic activity
90	IPI00307837.6	EEF1A1	Elongation factor 1-alpha 1	0.49	2.0E−04	Protein biosynthesis
91	IPI00462072.3	LOC100044223;	EG433182; eno1 alpha-enolase	0.48	3.1E−04	Metabolic enzymes, multifunctional enzyme (glycolysis, growth control, hypoxia tolerance and allergic responses), a receptor and activator of plasminogen
92	IPI00555069.3	PGK1	Phosphoglycerate kinase 1	0.48	9.2E−05	ATP + 3-phospho-D-glycerate = ADP + 3-phospho-D-glyceroyl phosphate
93	IPI00229080.7	HSP90AB1	Heat shock protein 84b	0.47	9.0E−04	Molecular chaperone
94	IPI00230139.5	FKBP4	FK506-binding protein 4	0.46	2.9E−02	Signal transduction, androgen receptor signaling pathway, copper ion transport, ATP binding, component of unactivated mammalian steroid receptor complexes, rotamase activity, the intracellular trafficking of heterooligomeric forms of steroid hormone receptors
95	IPI00225961.5	PHGDH	D-3-phosphoglycerate dehydrogenase	0.46	3.9E−06	3-phospho-D-glycerate + NAD^+ = 3-phosphonooxypyruvate + NADH 2-hydroxyglutarate + NAD^+ = 2-oxoglutarate + NADH
96	IPI00318841.4	EEF1G	Elongation factor 1-gamma	0.45	2.2E−03	Translation elongation factor activity
97	IPI00225201.5	IARS	Isoleucyl-tRNA synthetase, cytoplasmic	0.44	3.1E−04	ATP + L-isoleucine + tRNA(Ile) = AMP + diphosphate + L-isoleucyl-tRNA(Ile).
98	IPI00624863.1	PAICS	Phosphoribosylaminoimidazole carboxylase, phosphoribosylaminoribosylaminoimidazole, succinocarboxamide synthetase, full insert sequence	0.44	2.1E−02	Catalytic activity
99	IPI00407130.4	PKM2	Isoform M2 of pyruvate kinase isozymes M1/M2	0.43	0.0003	ATP biosynthetic process, glucose metabolic process
100	IPI00854035.1	LOC100047753	Similar to Nucleoside diphosphate kinase A	0.42	1.5E−03	The synthesis of nucleoside triphosphates, catalytic activity
101	IPI00469103.1	KARS	Lysyl-tRNA synthetase	0.40	2.4E−03	Catalytic activity
102	IPI00555113.2	RPl18	60S ribosomal protein L18	0.39	7.3E−03	Cellular structure
103	IPI00113223.2	FAS	Fatty acid synthase	0.363	3.69E−05	Fatty acid biosynthetic process [acyl-carrier-protein], *S*-acetyltransferase activity

(*Continued*)

TABLE II. (*Continued*)

Number	Accession	Gene	Protein	115:114	*P*-value, 115:114	Function
104	IPI00466069.3	EEF2	Elongation factor 2	0.33	7.0E−06	GTPase activity, GTP binding, this protein promotes the GTP-dependent translocation of the nascent protein chain from the A-site to the P-site of the ribosome
105	IPI00877279.1	ANXA3	Annexin A3	0.31	4.4E−03	Inhibitor of phospholipase A2, anti-coagulant properties
106	IPI00135189.3	AACS	Acetoacetyl-CoA synthetase	0.30	8.5E−05	Activates acetoacetate to acetoacetyl-CoA involved in utilizing ketone body for the fatty acid-synthesis during adipose tissue development

List of differential expressed proteins in adipocyte differentiation. A 115:114 is the ratio of different protein expression level in 3T3-LI adipocytes relative to 3T3-LI fibroblasts. The *P*-values indicated statistical significance of the observed differences, with $P < 0.05$ considered as statistically significant. In 115:114 column, an extra asterisk denotes a protein previously unknown to be involved with adipogenic process.

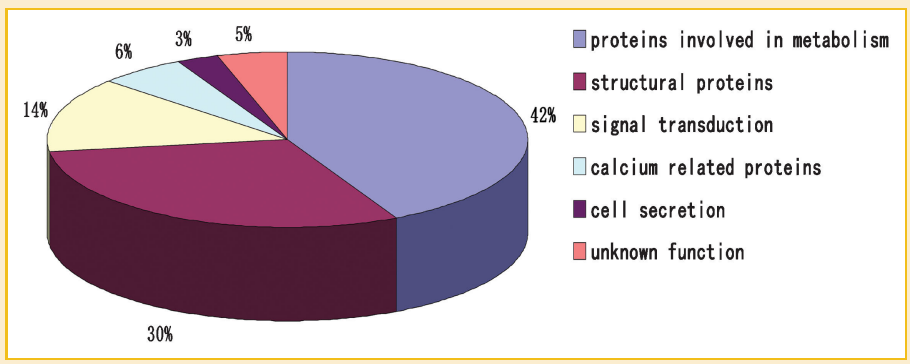

Fig. 1. Distribution of all altered proteins into different functional categories.

unchanged. In Table II, 11 proteins were altered threefold or more between pre-adipocyte and adipocyte, many changes agree with previous observations [Renes et al., 2005; Atiar Rahman et al., 2008; Kim et al., 2009; Molina et al., 2009; Choi et al., 2011]. We exemplified by LPL. LPL is an enzyme that hydrolyzes lipids in lipoproteins. It is activated by insulin in adipocytes, but both LPL and leptin has different secretory pathways. LPL is well-known as an adipocyte specific gene and significantly induced in fully differentiated adipocytes [Roh et al., 2001; Molina et al., 2009]. PPAR-gamma, a key component in the adipocyte differentiation, directly stimulates LPL expressions [Kawachi et al., 2007]. Our study demonstrated that LPL significantly increases, which is in agreement with previous studies [Roh et al., 2001; Molina et al., 2009]. However, some contradictory protein expression effects are found. FAS is a multi-enzyme that plays a key role in fatty acid synthesis. Interestingly, expression levels of FAS and PGK1 were significantly decrease, whereas PPAR-gamma expression was not significantly changes on day 10 of adipocyte differentiation, which are not consistent with previous studies [Hackl et al., 2005; Renes et al., 2005; Jitrapakdee et al., 2008]. We propose that different adipogenesis phases could be an important contributor to expression of the above proteins.

VERIFY DIFFERENTIALLY EXPRESSED PROTEINS BY WESTERN BLOT AND REAL-TIME PCR ANALYSIS

To assess if the protein changes as quantitated by iTRAQ coupled 2D LC/MS/MS were significant, Western blot analysis was carried out on nine proteins (Destrin; Nucleolin; Zyx protein; Transgelin 2; VDAC2; VDAC3; Cytochrome b5; PCX; and β-actin). All showed consistent results compared with their respective LC/MS-MS analysis. Similarly to the iTRAQ analysis, results shown in Figure 3 indicated that the level of proteins (Nucleolin; Transgelin 2; Destrin; and Zyx protein) were lower in adipocytes compared with the level in the control pre-adipocytes. Quantification of the proteins (Cytochrome b5; VDAC2; PCX; and VDAC3) showed significantly increased compared with the level in the control pre-adipocytes. Real-time PCR analysis of genes listed in Figure 4 was carried out to assess differentially expressed proteins. Significant changes were analyzed based on three independent experiments. These results are consistent with their respective LC/MS-MS analysis. The mRNA of genes (Cytochrome b5 and VDAC2) showed similar up-regulation in adipocytes. Results shown in Figure 4 indicated that down-regulated mRNA in adipocytes included Nucleolin, Transgelin 2, Annexin A1, Ribosomal protein SA and Eukaryotic translation elongation factor 1 alpha 1. Four proteins (Cytochrome b5, VDAC2, Nucleolin and Transgelin 2) were validated by both real-time PCR and Western blot. Our real-time PCR results were consistent with the Western blot analysis. These results confirm iTRAQ analysis at both gene and protein levels.

THE ASSOCIATION OF PCX AND VDAC2 WITH ADIPOCYTE DIFFERENTIATION

To study the functional roles of PCX and VDAC2 up-regulation in 3T3-LI adipocytes, cells were transfected with PCX or VDAC2

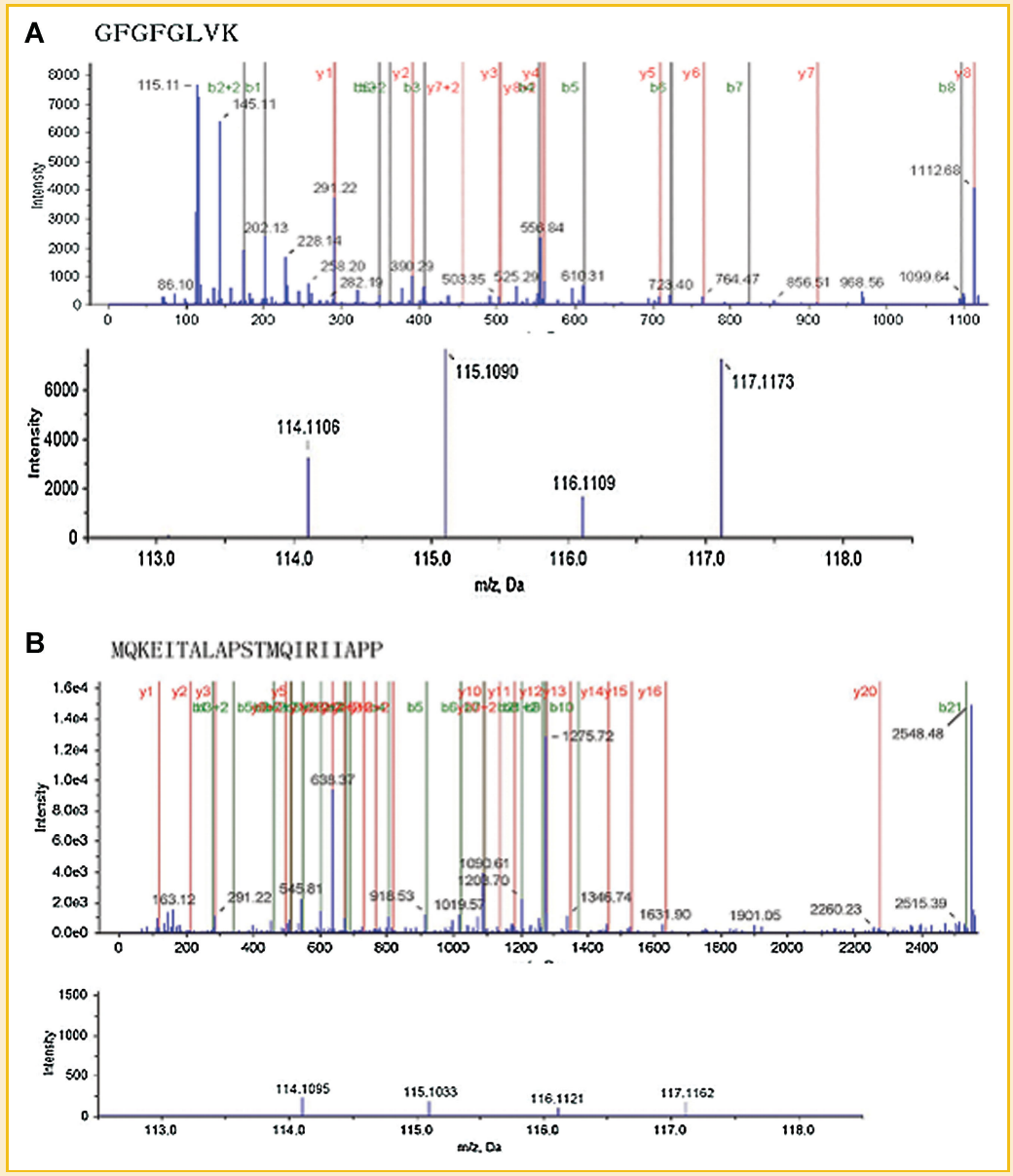

Fig. 2. A representative MS/MS spectrum showing the peptides from (A) VDAC2, (B) β-actin. The ion assignments are as follows: control 3T3-LI fibroblasts = iTRAQ 114; 3T3-LI adipocytes = iTRAQ 115. Compared with 3T3-LI fibroblasts, expression level of VDAC2 was significantly increased (A), whereas β-actin expressions was not significant changes (B) in 3T3-LI adipocytes.

siRNA. Firstly, siRNA-induced inhibitions of PCX or VDAC2 expression were determined by Western blot analysis. As shown in Figure 5A, PCX or VDAC2 siRNA significantly decreased PCX or VDAC2 protein levels, whereas PCX or VDAC2 protein expressions were not significantly suppressed by control siRNA. From our Western blot experiments, we observed that PCX and VDAC2 siRNAs silenced their targets by 33–45% and 40–50%, respectively (data not shown). We next evaluated the effect of PCX or VDAC2 siRNA transfection on adipogenic conversion. Differentiation of 3T3-L1 cells for 10 days resulted in an accumulation of triglyceride as shown by the red-colored cells, and Oil Red staining of triglyceride was almost not observed in control 3T3-L1 fibroblasts (Fig. 5B). These results were confirmed by measurement of the total amount of triglyceride and intracellular Oil Red staining (Fig. 5C,D). The content of triglyceride and intracellular Oil Red staining in differentiated 3T3-L1 adipocytes was strongly increased compared to pre-adipocytes. PCX or VDAC2 siRNA significantly reduced the content of triglyceride (by 73.7% and 76.1%) and intracellular Oil Red staining (by 66.7% and 69.8%).

DISCUSSION

The main findings of this study are; (1) a total number of 106 proteins differentially expressed were identified using iTRAQ-based proteomic approach, of them, 24 proteins have not been reported

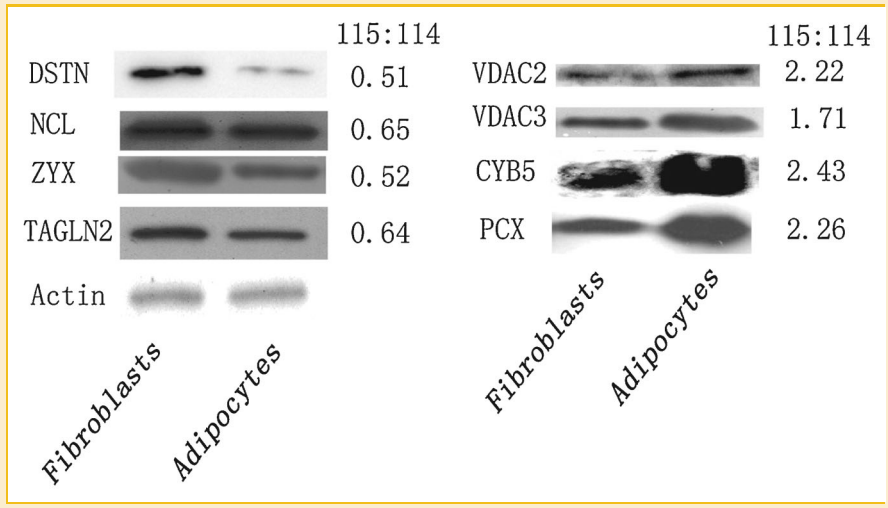

Fig. 3. Western blot analysis of protein levels of (1) Destrin; (2) Nucleolin; (3) Zyx protein; (4) Transgelin 2; (5) VDAC2; (6) VDAC3; (7) Cytochrome b5; (8) PCX; and (9) β-actin in 3T3-LI fibroblasts and adipocytes. β-Actin in the cell lysate served as a loading control.

before in 3T3-L1 adipocyte differentiation including HEXB, DPP7, PTTG1IP, PRDX5, EPDR1, SPNB2, STEAP3, NIBAN, ACADM, RPS19, NEDD4, KANK2, LOC10045699, EG432502, NUCB1, MBC2, FBN1, CALU, CAPG, VDAC1, VDAC3, 1300012G16Rik, HSPE1, and TPP1. (2) The association of PCX and VDAC2 with adipogenesis was verified, showing PCX siRNA and VDAC2 siRNA transfection could significantly inhibit 3T3-L1 adipocyte differentiation.

Compared with 2-DE technique, iTRAQ has several advantages such as high sensitivity in the detection of proteins in low concentrations and hydrophobic membrane proteins, good sample capacity, high reproducibility, and accurate quantitation [Hu et al., 2010; Zhang et al., 2011]. Using this method, we screened 106 differentially expressed proteins. The majority of differential proteins were related to metabolic enzymes and structural proteins. Among those differential metabolic enzymes, many were consistent with previous results [Zhang et al., 1995; Roh et al., 2001; Wilson-Fritch et al., 2003; Renes et al., 2005; Atiar Rahman et al., 2008; Molina et al., 2009], but seven were first discovered in 3T3-L1 differentiation. PCX is a regulatory metabolic enzyme that provides acetyl-CoA and NADPH for the de novo biosynthesis of fatty acids. Cellular expression of PCX was regulated by glucagon, glucocorticoids, insulin, and PPAR-gamma. PCX plays a role in lipogenesis and gluconeogenesis, in glucose-induced insulin secretion by pancreatic islets, and in the biosynthesis of neurotransmitters [Zhang et al., 1995; Jitrapakdee et al., 2005, 2008], and a 2.26 of fold change was found in this study which is in agreement with previous studies [Zhang et al., 1995; Wilson-Fritch et al., 2003]. Therefore, the possible role of PCX up-regulation in the adipocyte differentiation was further investigated by siRNA method. Oil Red staining and triglyceride results showed that PCX siRNA transfection could significantly inhibit adipogenesis, suggesting that PCX plays a pivotal role during adipocyte conversion. The function of PKM2 in adipose tissue remains poorly defined. However, the data from other cell species demonstrate that PKM2 plays an important role in cell proliferation. PKM2 is increased in proliferating cells [Li et al., 2010]. In addition, Christofk et al. [2008] applied RNAi to knock down PKM2 expression in H1299 cells, resulting in reduced glycolysis and decreased cell proliferation. Taken together with our data that low level of PKM2 was present in adipocyte differentiation, we suppose that most likely PKM2 suppressed adipogenesis. The down-regulation of PHGDH may decrease the exit of 3-phosphoglycerate from the glycolytic pathway and consequently stimulate the conversion of glucose into acetyl-CoA [Renes et al., 2005]. Additional, both FAS and LOC100044223 are involved in fatty acid

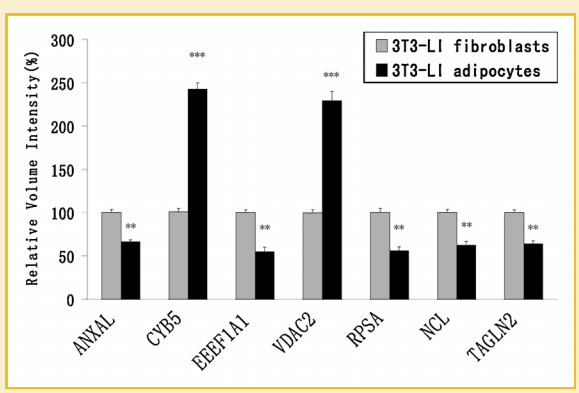

Fig. 4. Real-time PCR analysis of mRNA levels of (1) Annexin A1; (2) Cytochrome b5; (3) Eukaryotic translation elongation factor 1 alpha 1; (4) VDAC2; (5) Ribosomal protein SA; (6) Nucleolin; (7) Transgelin 2; (8) β-actin in 3T3-LI fibroblasts and adipocytes. Compared with 3T3-LI fibroblasts, 3T3-LI adipocytes had an obvious up-regulation of Cytochrome b5 and VDAC2 and down-regulation of Ribosomal protein SA, Eukaryotic translation elongation factor 1 alpha 1, Nucleolin, Transgelin 2, and Annexin A1, which were identical with the protein level changes in iTRAQ analysis. The statistics (mean ± SEM) was obtained from 3–4 experiments. The values normalize with β-actin mRNA levels. $^{*}P < 0.05$ considered as statistically significant. $^{**}P < 0.01$, $^{***}P < 0.001$ versus 3T3-LI fibroblasts.

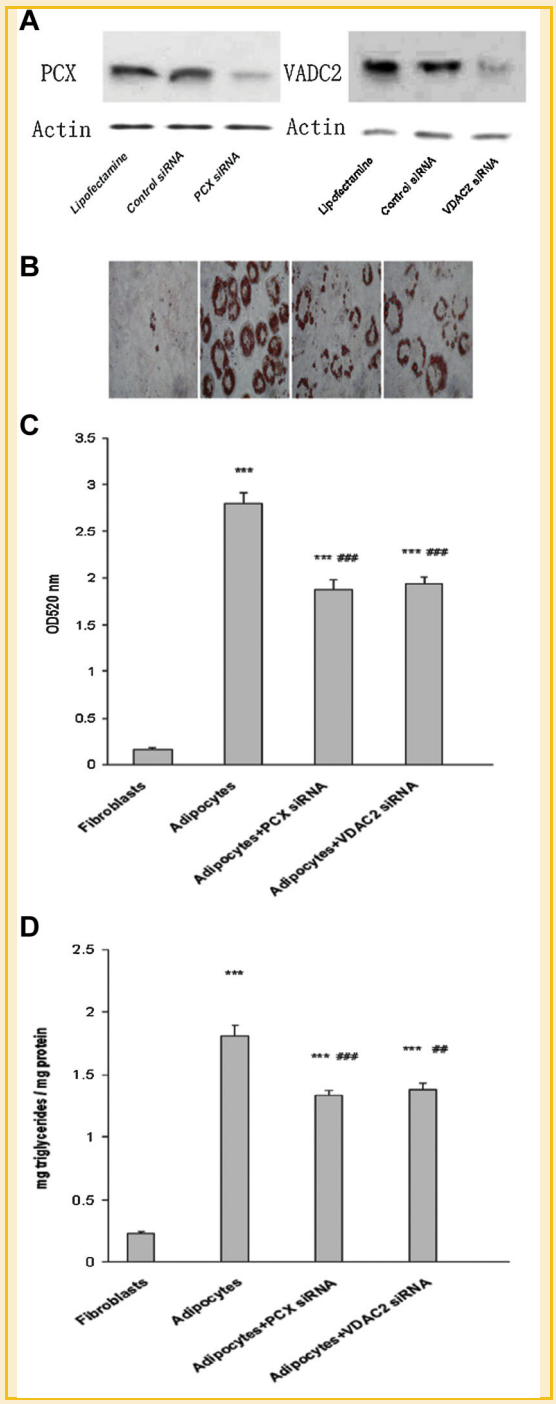

Fig. 5. A: Western blot analysis showed that transfection of 3T3-LI cells with PCX or VDAC2 siRNA significantly reduced PCX or VDAC2 protein levels, whereas PCX or VDAC2 protein expressions were not significantly suppressed by control siRNA and Lipofectamine 2000. β-Actin in the cell lysate served as a loading control. Lipofectamine 2000 (a cationic lipid, Invitrogen Corporation), cells treated with Lipofectamine 2000 only. B–D: Furthermore, Oil Red staining (B,C) and triglyceride assay (D) showed that transfection of 3T3-LI cells with PCX or VDAC2 siRNA could inhibit in adipocyte differentiation. Triglyceride was showed as mg cellular triglyceride per mg of total cellular protein. The experiments were repeated in triplicate. Values are mean ± SEM. $^{*}P < 0.05$ considered as statistically significant. $^{**}P < 0.01$, $^{***}P < 0.001$ versus 3T3-LI fibroblasts. $^{\#\#}P < 0.01$, $^{\#\#\#}P < 0.001$ versus 3T3-LI adipocytes.

synthesis and glycolytic activity [Jitrapakdee et al., 2008; Kang et al., 2008].

Here, we also observed a differential expression of structural proteins (including cytoskeletal proteins, molecular chaperone). Among them, the increased expression of FABP4 is in agreement with enhanced fatty acid synthesis [Kawachi et al., 2007; Karakas et al., 2009]. Voltage-dependent anion channels (VDACs) are a class of porin ion channel located on the outer mitochondrial membrane [Hoogenboom et al., 2007]. Vertebrates have at least three members (VDAC1, VDAC2, and VDAC3), and three mammalian isoforms may each have some distinct physiological role [Cheng et al., 2003]. VDAC proteins constitute the major pathway for metabolic exchange across mitochondrial outer membrane (MOM). Although neither VDAC2 protein levels nor mRNA levels were further validated, two studies indicated VDAC2 significantly increased in adipogenesis using cDNA microarray or 2-DE analysis [Tan et al., 2006; Kim et al., 2009]. Furthermore, our results agree with above-mentioned observations. Interestingly, our data show that all three members were markedly increased in adipogenesis, and VDAC2 showed the largest changes (2.22 of fold change) in protein expression among them. Whether increased VDAC2 is mechanistically related to adipocyte differentiation? To our best knowledge, it has not yet been reported. To study the functional role of VDAC2 up-regulation during adipocyte induction, 3T3-L1 cells were transfected with siRNA against VDAC2. We firstly demonstrated that the suppression of VDAC2 expression markedly inhibited adipocyte differentiation. Thus, it suggests that some structural proteins can contribute to adipogenesis. As we know that both VDAC2 and VDAC1 are components of the permeability transition pore complex (PTPC) of the mitochondrial inner and outer membranes, respectively. The subsequent dissipation of mitochondrial inner membrane potential and release of cytochrome *c* through the outer mitochondrial membrane are critical events in the early stages of apoptosis. VDACs have been proposed in several reports as a participant in cell death [Zamzami and Kroemer, 2001; Cheng et al., 2003; Yagoda et al., 2007]. Yagoda et al. [2007] indicated that ligands to VDACs induce non-apoptotic cell death selectively in some tumor cells harboring activating mutations in the RAS–RAF–MEK pathway. We suppose that VDAC2 is crucial in maintaining the viability of pre-adipocytes during adipogenesis, and decreased VDAC2 expression induces differentiating pre-adipocytes apoptosis. In additional, Cheng et al. [2003] consolidated that VDAC2, but not VDAC1 or VDAC3, significantly inhibited apoptosis mediated by BAK. Critical questions are what roles, if any, does these proteins play in adipogenesis, and whether would VDACs activate different signal pathways regulating adipogenesis? Further study will be necessary to fully understand the molecular events during adipogenic process. Another up-regulated cellular structure protein is cytochrome b5 which passes electrons from NADH, NADPH, and ascorbate to the cyanide-sensitive factor where fatty acid desaturation takes place. Reduced cytochrome b5 then provides reducing equivalents for the biosynthesis of selected lipids and drugs [Canova-Davis and Waskell, 1984; Stayton et al., 1988]. However, there have been few studies on the changes of adipose tissue cytochrome b5 contents in obesity. Previous studies suggested that cytoskeletal remodeling occurs during adipogenesis. Many

proteins such as Annexin, MYO1C, and Destrin are involved in differentiation process. Our study is similar with previous observations [Hackl et al., 2005; Renes et al., 2005; Molina et al., 2009]. Previous study indicated that cytoskeletal remodeling does not hinder lipolysis [Brasaemle et al., 2000]. However, the behavior of the cytoskeleton remains obscure during 3T3-L1 differentiation. Other interesting proteins include CCT4, CCT8, HSPE1, and HSP90AB1. Although underlying mechanisms remain to be further elucidated, the expression levels of these four molecular chaperones were decreased in adipocyte.

Among 15 differential proteins involved in signal transduction (including growth-regulator), several proteins such as C/EBPs and CREB were consistent with previous observations, but three proteins involved in secretion (EPDR1, SPNB2, and STEAP3) were first discovered in 3T3-L1 differentiation. EPDR1, a soluble transmembrane protein, is secreted from mouse fibroblasts too [Sleat et al., 2006]. It was reported to be associated with extracellular matrix too [Shashoua et al., 1990]. SPNB2 is involved in secretion. It also interacts with calmodulin in a calcium-dependent manner and is thus a candidate for the calcium-dependent movement of the cytoskeleton at the membrane [Urzua et al., 2006]. STEAP3 shown to facilitate the secretion of translationally controlled tumor protein (TCTP) through a non-classical pathway [Amzallag et al., 2004]. However, the adipogenesis mechanisms involve these proteins have not been elucidated. These questions remain to be further elucidated.

A total number of six calcium-related proteins differentially expressed were showed. The calcium ion is a highly versatile intracellular signal regulating many different cellular functions [Bootman and Berridge, 1995]. Transient calcium signals are transduced by calcium-binding proteins acting on downstream effector proteins and various enzymes. The calcium-related protein plays a crucial role in various cellular signaling cascades through regulation of numerous target proteins in a calcium-dependent manner. However, little is known about the roles of calcium-related proteins during adipogenesis.

Our results reveal changes in the profile of 106 protein species. Moreover, we found 24 proteins whose expression has not been reported before in 3T3-L1 adipocyte differentiation, and association of PCX and VDAC2 with adipogenesis was verified. The complex etiology of obesity requires a full understanding of the molecular events during adipogenesis. These data provide new targets for future investigation studies with respect to obesity.

ACKNOWLEDGMENTS

This work was supported by Natural Sciences Funds of China (30971532, 30771134, 30930082, 30900507, and 30801348).

REFERENCES

Akerblad P, Mansson R, Lagergren A, Westerlund S, Basta B, Lind U, Thelin A, Gisler R, Liberg D, Nelander S, Bamberg K, Sigvardsson M. 2005. Gene expression analysis suggests that EBF-1 and PPARgamma2 induce adipogenesis of NIH-3T3cells with similar efficiency and kinetics. Physiol Genomics 23:206–216.

Amzallag N, Passer BJ, Allanic D, Segura E, Thery C, Goud B, Amson R, Telerman A. 2004. TSAP6 facilitates the secretion of translationally controlled tumor protein/histamine-releasing factor via a nonclassical pathway. J Biol Chem 279:46104–46112.

Atiar Rahman M, Kumar SG, Lee SH, Hwang HS, Kim HA, Yun JW. 2008. Proteome analysis for 3T3-L1 adipocyte differentiation. J Microbiol Biotechnol 18:1895–1902.

Bootman MD, Berridge MJ. 1995. The elemental principles of calcium signaling. Cell 83:675–678.

Bornstein SR, Abu-Asab M, Glasow A, Path G, Hauner H, Tsokos M, Chrousos GP, Scherbaum WA. 2000. Immnohistochemical and ultrastructural localization of leptin and leptin receptor in human white adipose tissue and differentiating human adipose cells in primary culture. Diabetes 49:532–538.

Brasaemle DL, Levin DM, Adler-Wailes DC, Londos C. 2000. The lipolytic stimulation of 3T3-L1 adipocytes promotes the translocation of hormone-sensitive lipase to the surfaces of lipid storage droplets. Biochim Biophys Acta 1483:251–262.

Bray GA, Tartaglia LA. 2000. Medicinal strategies in the treatment of obesity. Nature 404:672–677.

Canova-Davis E, Waskell L. 1984. The identification of the heat-stable microsomal protein required for methoxyflurane metabolism as cytochrome b5. J Biol Chem 259:2541–2546.

Cheng EH, Sheiko TV, Fisher JK, Craigen WJ, Korsmeyer SJ. 2003. VDAC2 inhibits BAK activation and mitochondrial apoptosis. Science 301:513–517.

Choi KL, Wang Y, Tse CA, Lam KS, Cooper GJ, Xu A. 2004. Proteomic analysis of adipocyte differentiation: Evidence that alpha2 macroglobulin is involved in the adipose conversion of 3T3 L1 preadipocytes. Proteomics 4:1840–1848.

Christofk HR, Vander Heiden MG, Wu N, Asara JM, Cantley LC. 2008. Pyruvate kinase M2 is a phosphotyrosine-binding protein. Nature 452: 181–186.

Cock TA, Auwerx J. 2003. Leptin: Cutting the fat off the bone. Lancet 362: 1572–1574.

Hackl H, Burkard TR, Sturn A, Rubio R, Schleiffer A, Tian S, Quackenbush J, Eisenhaber F, Trajanoski Z. 2005. Molecular processes during fat cell development revealed by gene expression profiling and functional annotation. Genome Biol 6:R108.

Hoogenboom BW, Suda K, Engel A, Fotiadis D. 2007. The supramolecular assemblies of voltage-dependent anion channels in the native membrane. J Mol Biol 370:246–255.

Hu HD, Ye F, Zhang DZ, Hu P, Ren H, Li SL. 2010. iTRAQ quantitative analysis of multidrug resistance mechanisms in human gastric cancer cells. J Biomed Biotechnol 2010:571343.

Jitrapakdee S, Slawik M, Medina-Gomez G, Campbell M, Wallace JC, Sethi JK, O'Rahilly S, Vidal-Puig AJ. 2005. The peroxisome proliferator-activated receptor-gamma regulates murine pyruvate carboxylase gene expression in vivo and in vitro. J Biol Chem 280:27466–27476.

Jitrapakdee S, St Maurice M, Rayment I, Cleland WW, Wallace JC, Attwood PV. 2008. Structure, mechanism and regulation of pyruvate carboxylase. Biochem J 413:369–387.

Kang HJ, Jung SK, Kim SJ, Chung SJ. 2008. Structure of human alpha-enolase (hEN01), a multifunctional glycolytic enzyme. Acta Crystallogr D Biol Crystallogr 64:651–657.

Karakas SE, Almario RU, Kim K. 2009. Serum fatty acid binding protein 4, free fatty acids, and metabolic risk markers. Metabolism 58:1002–1007.

Kawachi H, Moriya NH, Korai T, Tanaka SY, Watanabe M, Matsui T, Kawada T, Yano H. 2007. Nitric oxide suppresses preadipocyte differentiation in 3T3-L1 culture. Mol Cell Biochem 300:61–67.

Kim SH, Park HS, Lee MS, Cho YJ, Kim YS, Hwang JT, Sung MJ, Kim MS, Kwon DY. 2008. Vitisin A inhibits adipocyte differentiation through cell cycle arrest in 3T3-L1cells. Biochem Biophys Res Commun 372:108–113.

Kim KB, Kim BW, Choo HJ, Kwon YC, Ahn BY, Choi JS, Lee JS, Ko YG. 2009. Proteome analysis of adipocyte lipid rafts reveals that gC1qR plays essential

roles in adipogenesis and insulin signal transduction. Proteomics 9:2373–2382.

Lago F, Dieguez C, Gomez-Reino J, Gualillo O. 2007. Adipokines as emerging mediators of immune response and inflammation. Nat Clin Pract Rheumatol 3:716–724.

Lago F, Gomez R, Gomez-Reino JJ, Dieguez C, Gualillo O. 2009. Adipokines as novel modulators of lipid metabolism. Trends Biochem Sci 34:500–510.

Li SL, Ye F, Cai WJ, Hu HD, Hu P, Ren H, Zhu FF, Zhang DZ. 2010. Quantitative proteome analysis of multidrug resistance in human ovarian cancer cell line. J Cell Biochem 109:625–633.

Miner JL. 2004. The adipocyte as an endocrine cell. J Anim Sci 82:935–941.

Molina H, Yang Y, Ruch T, Kim JW, Mortensen P, Otto T, Nalli A, Tang QQ, Lane MD, Chaerkady R, Pandey A. 2009. Temporal profiling of the adipocyte proteome during differentiation using a five-plex SILAC based strategy. J Proteome Res 8:48–58.

Renes J, Bouwman F, Noben JP, Evelo C, Robben J, Mariman E. 2005. Protein profiling of 3T3-L1 adipocyte differentiation and (tumor necrosis factor alpha-mediated) starvation. Cell Mol Life Sci 62:492–503.

Roh C, Roduit R, Thorens B, Fried S, Kandror KV. 2001. Lipoprotein lipase and leptin are accumulated in different secretory compartments in rat adipocytes. J Biol Chem 276:35990–35994.

Rondinone CM. 2006. Adipocyte-derived hormones, cytokines, and mediators. Endocrine 29:81–90.

Rosen ED, Spiegelman BM. 2006. Adipocytes as regulators of energy balance and glucose homeostasis. Nature 444:847–853.

Shao DL, Lazar MA. 1997. Peroxisome proliferator activated receptor gamma, CCAAT/enhancer-binding protein alpha, and cell cycle status regulate the commitment to adipocyte differentiation. J Biol Chem 272: 21473–21478.

Shashoua VE, Hesse GW, Milinazzo B. 1990. Evidence for the in vivo polymerization of ependymin: A brain extracellular glycoprotein. Brain Res 522:181–190.

Sleat DE, Zheng H, Qian M, Lobel P. 2006. Identification of sites of mannose 6-phosphorylation on lysosomal proteins. Mol Cell Proteomics 5:686–701.

Stayton PS, Fisher MT, Sligar SG. 1988. Determination of cytochrome b5 association reactions. Characterization of metmyoglobin and cytochrome P-450cam binding to genetically engineered cytochrome b5. J Biol Chem 263:13544–13548.

Tan SH, Reverter A, Wang Y, Byrne KA, McWilliam SM, Lehnert SA. 2006. Gene expression profiling of bovine in vitro adipogenesis using a cDNA microarray. Funct Integr Genomics 6:235–249.

Than A, Ye F, Xue R, Ong JW, Poh CL, Chen P. 2010. The crosstalks between adipokines and catecholamines. Mol Cell Endocrinol 332:261–270.

Thompson D, Wolf AM. 2001. The medical-care cost burden of obesity. Obes Rev 2:189–197.

Trujillo ME, Scherer PE. 2006. Adipose tissue-derived factors: Impact on health and disease. Endocr Rev 27:762–778.

Urzua U, Roby KF, Gangi LM, Cherry JM, Powell JI, Munroe DJ. 2006. Transcriptomic analysis of an in vitro murine model of ovarian carcinoma: Functional similarity to the human disease and identification of prospective tumoral markers and targets. J Cell Physiol 206:594–602.

Wilson-Fritch L, Burkart A, Bell G, Mendelson K, Leszyk J, Nicoloro S, Czech M, Corvera S. 2003. Mitochondrial biogenesis and remodeling during adipogenesis and in response to the insulin sensitizer rosiglitazone. Mol Cell Biol 23:1085–1094.

Yagoda N, von Rechenberg M, Zaganjor E, Bauer AJ, Yang WS, Fridman DJ, Wolpaw AJ, Smukste I, Peltier JM, Boniface JJ, Smith R, Lessnick SL, Sahasrabudhe S, Stockwell BR. 2007. RAS-RAF-MEK-dependent oxidative cell death involving voltage-dependent anion channels. Nature 447:864–868.

Ye F, Than A, Zhao YY, Goh KH, Chen P. 2010. Vesicular storage, vesicle trafficking, and secretion of leptin and resistin: The similarities, differences, and interplays. J Endocrinol 206:27–36.

Zamzami N, Kroemer G. 2001. The mitochondrion in apoptosis: How Pandora's box opens. Nat Rev Mol Cell Biol 2:67–71.

Zhang J, Xia WL, Ahmad F. 1995. Regulation of pyruvate carboxylase in 3T3-L1cells. Biochem J 306(Pt 1): 205–210.

Zhang H, Zhao C, Li X, Zhu Y, Gan CS, Wang Y, Ravasi T, Qian PY, Wong SC, Sze SK. 2011. Study of monocyte membrane proteome perturbation during lipopolysaccharide-induced tolerance using iTRAQ-based quantitative proteomic approach. Proteomics 10:2780–2789.

Zhou YT, Wang ZW, Higa M, Newgard CB, Unger RH. 1999. Reversing adipocyte differentiation: Implications for treatment of obesity. Proc Natl Acad Sci USA 96:2391–2395.